INSPECTION INTERVAL FOR TENDON JOINTS OF JOLLIET TLP

Gudfinnur Sigurdsson
Det Norske Veritas
Høvik
Norway

Jan Mathisen
Det Norske Veritas
Høvik
Norway

Stephen Bultema
Conoco Inc.
Houston
USA

ABSTRACT

A reliability analysis is developed for the welded joints of the tendons on the Jolliet TLP. Two potential failure modes are considered: (a) fatigue failure in terms of growth of a fatigue crack through the tendon wall thickness, and (b) rupture due to brittle fracture or plastic collapse in the presence of a fatigue crack. Linear fracture mechanics are used to model the growth of a fatigue crack. Final rupture is modelled using a failure assessment diagram approach defined in PD6493 (from BSI, 1997). Material data from the production testing of the tendons are applied. Initial crack sizes are based on measurements made during the initial in-service inspection carried out in 1989/90. Extreme load distributions are based on the original design analyses of the TLP, while fatigue loads are based on in-service measurements. Axial tension and transverse bending moments at the tendon joint are included in both cases.

The annual probability of failure is computed as a function of the time elapsed since the inspection. Both failure modes and the combination of the two failure modes are considered. Comparison of these results with a suitable target reliability level is used to evaluate when the next inspection of the tendon joint welds should be performed.

BACKGROUND

This paper addresses the long term integrity of the mooring system of the Jolliet TLP and the need for inspection. Jolliet is located on Green Canyon Block 184 in the Gulf of Mexico. The Tension Leg Well Platform (TLWP) was installed at this location during the latter half of 1989 (ref. Wybro et al.). It is moored with 12 single piece tendons, 3 per corner, and 512 m (1680 ft) long. They are made up from 12.2m (40-ft) sections of TMCP pipe with 35 circumferential welds along the length.

This installation was the first of a kind within the Gulf of Mexico and first under the jurisdiction of the United States Coast Guard and the Minerals Management Services. The nature of this convinced Conoco to develop an inspection program that was consistent with API RP2T (1987). Prior to the platform installation, the USCG/MMS and Conoco agreed to the proposal. The agreement set the interval for inspection to once every 4-years with a baseline in-situ inspection to take place within the first 2 years of the platform installation.

The initial in-situ baseline internal tendon inspection was completed in 1991 and this is the work that will be referenced within this paper. The inspection provided sufficient information to allow Conoco to request some relief in the original 4-year inspection interval. In 1993, the USCG agreed and Conoco was allowed to defer the first inspection until 1999 and every 8 years thereafter.

Between the years of 1994-1996, Conoco sponsored a research program (CNRD 1-62). The study employed DNV to work on the development of fatigue and final fracture mechanics of TLP tendons and assess the reliability of this type of mooring system. As part of this work the methodology was applied to the Hutton tendons as a verification of the fatigue and failure probability for this TLP (ref. Mathisen and Sigurdsson, 1996). These results were very encouraging and suggested that a similar analysis could be performed for Jolliet (ref. Sigurdsson and Mathisen, 1998). The work, as presented herein, would focus on determining the fatigue life and use fracture mechanics to evaluate crack growth in the planar indications found during the initial in-situ inspection. The goal of the work was to determine the requirement for inspection.

During tendon fabrication Conoco had a zero defect allowance. To insure weld quality all welds were inspected at the yard using MPI, UT and Radiography. As each tendon was fabricated it was documented and any imperfection discovered in the weld was ground out and the location re-welded. This is a practice which is carried out today for all welds on all tendons for the TLPs in the Gulf of Mexico. After fabrication the tendons were lifted from land to quayside and from there towed to site, upended and installed.

A great deal of design and analysis was performed in order to develop a tool which was capable of giving a reliable inspection. The tool that was developed used UT and was run internally to investigate each of the 35 welds in each of the 12 tendons. In all 10 planar indications were recorded. The two most severe have been the focus of this paper.

TENDON MATERIAL DATA AND IN-SITU INSPECTION FINDINGS

The tendon dimension and tendon material properties are based on testing results of the Jolliet tendons. The test results which are found relevant for the current study are presented in the following table, Summary Report of Conoco Tendon Pipe (1988).

Pipe property	N*	Mean value	unit	CoV	Assumed dist.
yield stress weld metal **	23	493	MPa	0.016	Normal
ultimate tensile strength weld metal **	23	584	MPa	0.014	Normal
Outside Diameter	36	610	mm	≈ 0	Fixed
Wall thickness	36	20.7	mm	0.005	Fixed
Charpy Energy ** weld metal at -30^o F	657	213	Nm	0.09	Weibull
Charpy Energy ** HAZ at -30^o F	657	199	Nm	0.15	Weibull

* Number tests/measurements
** Transverse direction

The variabilities of the outer diameter and the wall thickness are very small and these dimensions can be assumed to be deterministic. Also the variabilities in the yield strength and the ultimate tensile strength are small. The variability in the Charpy value is, however, significant and will be modelled as stochastic property. The mean Charpy value is lower and the variability is significantly larger for the HAZ than in the weld material. Therefore, the properties obtained for the HAZ will be used in the reliability analysis. The Weibull distribution has been shown to provide a good fit to the test results.

The first in-situ Inspection of the Jolliet tendons was successfully carried out during the period from October 2, 1990 to November 4, 1990 and completed during the period from May 28, 1991 to August 14, 1991. Ten non-geometrical flaw indications were observed. All except one of the non-geometrical flaw findings are on the inner surface. One volumetric flaw has been observed. The size of the largest surface breaking flaw indication was 4.78 mm deep and 17.8 mm long. The length of the volumetric flaw indication is 127mm. This indication is a surface reflector that is not surface connected. The through wall dimension is stated as negligible (< 1.2 mm) and the indication is located at 3.9mm below the inner surface. This flaw will conservatively be assumed as a surface crack with depth equal to 1.21 mm. The flaw indications mentioned above have been considered in the probabilistic analysis.

The sizing accuracy for the applied sizing technique for the tendon inspection has been quantified as unbiased, normally distributed, with a standard deviation of about 1.3 mm.

ANALYSIS OVERVIEW

This analysis is concerned with the probability of failure of a welded joint, in a TLP tendon, in a specific time interval. Two failure modes are considered:

1. Fatigue crack growth through the tendon wall, and
2. tendon rupture under extreme loads, in the presence of a fatigue crack.

Physical models for the loads, the crack growth process, and the resistance to rupture are briefly described below. These models are assembled, together with their respective uncertainties, and used to compute the probability of either failure mode in various time intervals. This information is used to assess the need for inspection of the tendon joints during the remaining platform life.

Load Model

Fig. 1 shows the general arrangement of the Jolliet TLP. More details are given by Hunter et al (1990), Koon and Langewis (1990), and Hein et al. (1990). All the tendons are identically designed and constructed from butt-welded pipe segments. The diameter is 61 cm (24 in), the wall thickness is 2.06 cm. The environmental conditions at the site tend to induce the largest loads in the tendons attached to column number 3, at the West corner of the platform. The load model is primarily based on the centre tendon in the group of three attached to this column.

The excess buoyancy of the platform induces an important load component in the tendons, namely the pretension $p_{pre} = 3.412 \times 10^6$ N. The tendon ends are connected to flexible joints intended to reduce the bending moments induced in the tendons by platform offset. The tendons are designed with neutral buoyancy to avoid static imbalance effects when offset from the vertical. Platform motions in wave-frequency, low-frequency and high-frequency bands, and mean displacements may induce tendon loads. Local hydrodynamic actions on the tendons can also induce some load in the tendons. Lateral tendon dynamics have to be considered for tendons of this length. Both tendon tension and bending moment have to be considered in the crack growth process and for the rupture event. In general, the loads vary to some extent along the length of a tendon, and the effect of the bending moment varies around the tendon cross-section. The present study is limited to analysis of individual tendon joints, thus avoiding any need to model the stochastic dependencies between loads at various locations.

Extreme Load Distribution

The distribution of extreme tendon loads is required for analysis of the rupture event. This distribution is adapted from the results of the original design analysis by Combustion Eng. et al (1987). Total tendon tensions, at the most unfavourable position were computed for a number of environmental states. Interpolation on these results is applied to obtain tendon tensions for hurricane events with 5, 25, 50 and 100 year return periods. The following Gumbel distribution function is fitted to these data for the annual extreme tension

$$F_{P_{env}}(p_{env}) = \exp\left[-\exp\{-a(p_{env}-b\}\right] \quad (1)$$

where $a = 1.05\times10^{-6}$; $b = 1.18\times10^{6}$ using Newtons as units, and the total tension P is obtained as the sum of the environmental tension P_{env} and the pretension P_{pre}

$$p = p_{pre} + p_{env} \quad (2)$$

Note that the convention of using a lower case letter for realisations of a stochastic variable and the corresponding upper case letter for the stochastic variable itself is widely applied in this paper.

The highest total tensions occur at the top of the tendon and fall off to about 85% at mid-depth.

Quasi-static analysis is used to develop a model for the bending moment associated with the tension. A given value of platform offset implies a corresponding angle of rotation of the flex-joint at the top of the tendon, assuming the tendon does not bend. The flex-joint stiffness leads to the corresponding bending moment. Full correlation is assumed between tendon tension and platform offset, and a linear plus quadratic model is fitted to data for tension and offset from the original design analysis. This leads to the following expression for the bending moment associated with a given tension

$$m = 1701\left(d_1\, p_{env} + d_2\, p_{env}^2 + e\right) \text{ Nm} \quad (3)$$

where $d_1 = 9.65\times10^{-6}$ m/N, $d_2 = 0.57\times10^{-12}$ m/N^2 and e is a random error, with no bias and a standard deviation of 7.1 m. Comparison of this quasi-static model with results from the original design analysis including lateral tendon dynamics by Lumus Crest et al (1987a), indicate that this quasi-static model is conservative by about 30%.

A model uncertainty factor with a coefficient of variation of 15% is adopted for the extreme tension, since this is based on the original design analysis.

Fatigue Load Distribution

The long term distribution of stress ranges is required for the fatigue crack growth analysis. This is based on the measured in-service response of the tendons. The Jolliet TLP is fitted with an extensive instrumentation, including extensiometers on all tendons, at about 9 m below the top load-face. Standard deviations of tendon tensions have been stored for each 20 minute interval from 1989 to 1994. A Weibull distribution has been fitted to these tension standard deviations, from the most heavily-loaded tendon. It is assumed that the tendon tension is dominated by the wave-frequency response component at a mean period of 6 sec. On this basis, a Rayleigh distribution may be applied to describe the short term distribution of the tension ranges corresponding to each individual measured standard deviation. The theorem of total probability is then applied to obtain the long term distribution of the tension ranges P_R. This integration is performed using the PROBAN (DNVS, 1993) program, and the following Weibull distribution is fitted to the results

$$F_{P_R}(p_R) = 1 - \exp\left\{-\left(\frac{p_R - g_{P_R}}{a_{P_R}}\right)^{b_{P_R}}\right\} \quad (4)$$

with parameters $a_{P_R} = 6.33\times10^{4}$ N, $b_{P_R} = 0.9383$, $g_{P_R} = 0$ N.

In addition to the standard deviations, the instrumentation system also stores time histories from storms and other selected intervals. Some of these time histories have been analysed. Spectral analysis shows that there is a significant high-frequency component of tendon tension at about 0.45 Hz under typical operating conditions. However, the stresses induced by this tension component tend to lie below the fatigue threshold. Furthermore, when weather worsens and the loads increase, then the wave-frequency component dominates the tension response. The low-frequency component of tension is relatively negligible in both cases. These observations tend to justify the assumption of dominant wave-frequency response, made above.

Bending moments about two orthogonal axes are also available from the instrumentation system. These data have been used to study the ratio of normal stress to axial stress at various locations around the tendon wall. The normal stress includes both the longitudinal stresses due to bending moment and tension, while the axial stress is due to tension only. The oscillatory stress ratio is defined as the ratio of normal stress to axial stress at the most unfavourable position around the tendon wall. Sample results for the oscillatory stress ratio are shown plotted in Fig. 2. An average stress ratio of 1.45 is estimated from Fig. 2 for normal stresses exceeding 1.5 MPa (which is less than the fatigue threshold). This ratio applies provided the most unfavourable position in the tendon wall is considered, with respect to the heading of the environmental actions at that time. When the long term distribution of the environmental headings at the site is taken into account, the ratio is reduced to 1.3 – for the most unfavourable position in the tendon wall, in the long term. This oscillatory stress ratio is used to model the effect of bending moments on the crack growth process. It would not be applicable to extreme loads, because mean stresses are not included in the ratio.

The original dynamic analysis of the tendons by Lumus Crest et al (1987a,b) showed several bending modes to be present, and relatively little variation in the computed fatigue life along the length of the tendon: 801 years at the lowermost station, 627 years near the middle, and 638 years near the top. Hence, fatigue loads based on the extensiometers located near the top of the tendon should be reasonably applicable, over the whole tendon length, and conservative for the lower part of the tendon.

Since the fatigue loads are based on measurements, they are expected to be relatively accurate. A coefficient of variation of 10% is applied for the model uncertainty factor on the tension ranges.

Stress Concentration Factors

Mismatch Geometric SCF

The stress concentrations at tubular butt weld connections are due to eccentricities resulting from different sources. Normally the eccentricity due to out of roundness is giving the largest contribution to the resulting eccentricity. In ref. NORSOK (1999) the stress concentration factor (SCF) for tubular butt weld connections, due to eccentricities, is given as

$$SCF_{ecc} = 1 + 3.30\frac{e}{L}\sqrt{\frac{D}{t}}\exp(-a)\sin(a)$$

where D is the outer diameter, t is the wall thickness, L and e are defined in the Fig. 3 and α is given by

$$a = \frac{0.91L}{\sqrt{Dt}}$$

The maximum out-of-roundness per the tendon material specification is 1% of the diameter, which leads to difference in the tendon outer diameter of about 6 *mm*. The worst-case scenario occurs when the minor axis of one tubular is aligned with the major axis of the other tubular to which it is welded. The eccentricity will cause a local-bending moment in the tubular wall adjacent to the mismatch. This leads to an SCF_{ecc} of 1.72 (D = 610 *mm*, t = 20.7 *mm*, $L \cong 1.15t$) at the outer surface. The probability for this worst-case scenario at the joint under consideration is rather low and by assuming SCF_{ecc} = 1.72 will lead to over conservative results. Eccentricity in the magnitude of 3 – 4 *mm* are found more realistic values, which lead to *SCF* of 1.36 – 1.48.

In the reliability analysis the SCF_{ecc} is modelled as a normally distributed stochastic variable with a mean value of 1.4 and CoV of 10%.

Notch SCF at Weld Toe

The "as welded" crown profile will result in a notch SCF_{notch} located at the weld toe. This notch SCF_{notch} is located about the weld toe area and decays rapidly with the distance from the toe. The decay occurs along the outside surface of the tendon as well as with distance through the wall thickness. The SCF_{notch} depends on the stress distribution through the wall thickness and the weld geometry. The stress distribution through the wall thickness depends on the magnitude of the local bending stresses as well; i.e. the SCF caused by the eccentricity (SCF_{ecc}). The model proposed in BSI (1997) PD 6493 is applied for the current study.

Capacity Model

Crack-Growth Model

The growth of a fatigue crack is based on the Paris and Erdogan equation. A semi-elliptic crack shape is assumed such that the 2-dimensional differential equations for the increments in the crack size due to a load cycle are given by

$$\frac{da}{dN} = C_A(\Delta K_A)^m \;;\quad \Delta K_A > \Delta K_{th} \;;\quad a(N_0) = a_0 \tag{5}$$

$$\frac{dc}{dN} = C_C(\Delta K_C)^m \;;\quad \Delta K_C > \Delta K_{th} \;;\quad c(N_0) = c_0 \tag{6}$$

where a is the crack depth, $2c$ is the crack length, N indicates the load-cycle number, C_A, C_C, m are material parameters, $\Delta K_A, \Delta K_C$ are ranges of stress intensity factors for a specific load cycle, subscript *th* indicates a threshold level of stress intensity range below which the crack does not grow, and subscript *0* indicates the initial crack size. The material property m is assumed to be independent of the crack size. The material properties C_A, C_C may differ due to the general triaxial stress field. The relationship proposed by Raju and Newman (1981) and by Shang-Xian (1985) is also adopted here

$$C_A = 1.1^m\, C_C \tag{7}$$

It is usual to solve the differential equations for a given critical crack size. They may be rewritten as follows for this purpose

$$\frac{dc}{da} = \frac{C_C}{C_A}\left(\frac{\Delta K_C}{\Delta K_A}\right)^m \quad ;\quad c(a_0) = c_0 \tag{8}$$

$$\frac{dN}{da} = \frac{1}{C_A(\Delta K_A)^m} \quad ;\quad N(a_0) = N_0 \tag{9}$$

A standard algorithm for ordinary differential equations is applied to obtain the number of load cycles and the corresponding crack length for a given critical crack depth. The following general expression for the stress-intensity factor is inserted in equations (8) and (9)

$$K = \underline{Y} \cdot S_{tot}\sqrt{pa} \tag{10}$$

where S_{tot} is the applied stress and $\underline{Y}$ is the geometry function accounting for the effect of all the boundaries. Empirical equations for the stress intensity factor, for a surface crack in a finite plate subjected to membrane and bending loads, are applied according to Newman and Raju (1981). It is also assumed that the ratio of bending stress to membrane stress may be taken as a fixed value, ref. Sigurdsson and Torhaug (1993).

The following additional parameters are applied in the crack-growth analysis:

Material parameter m:
deterministic, m=2.67

Material parameter C:
$\text{Log}_{10}C$ is normally distributed, with mean –11.222 and standard deviation 0.264.

Stress intensity threshold:
deterministic, $\Delta K_{th} = 63\ \text{N/mm}^{3/2}$

Model uncertainty factor on geometry function:
normally distributed with coefficient of variation = 0.1.

Number of stress ranges per second: 0.15.

Rupture Model

Final rupture is evaluated by applying the failure assessment diagram (FAD) method (BSI 1997), in which a failure assessment curve (FAC) defines the boundary between safe and unsafe conditions. The condition of the assessed component is described by two parameters defining the assessment point; one parameter K_r reflecting the condition with respect to unstable fracture according to linear elastic fracture mechanics, and one parameter L_r reflecting the condition with respect to plastic collapse. Safe conditions are predicted if the assessment point is located within the assessment curve. The FAD method is intended to predict initiation of both brittle and ductile fracture. Fig. 4 shows an example of a failure assessment diagram, also illustrating the modelling of uncertainty in the failure assessment curve. With the data available, the failure assessment curve referred to as "Option 1 of Rev.3 of the R-6 method" is applied:

$$K_r = (1 - 0.14L_r^2)\left\{0.3 + 0.7\exp(-0.65L_r^6)\right\} \tag{11}$$

When an assessment point is computed, the subscript a is appended as a reminder that the Applied loads are considered.

$L_{r,a}$ is defined as the ratio of the effective stress on the section of material adjacent to the crack under consideration, relative to the flow strength of the material, and

$K_{r,a}$ is defined as the ratio of the applied stress intensity factor to the material fracture toughness (which may be calculated from the critical stress intensity factor or the critical CTOD) plus the effect of interaction between primary and secondary stresses. The applied stress intensity is computed as for the crack-growth model, taking account of the total membrane and bending stress, rather than the cyclic stress range. The plastic collapse parameter $L_{r,a}$ is obtained from the ratio of the applied loading to the limit loading. The lower-bound theorem of plasticity is applied to obtain a conservative estimate of the tendon limit loading. The model given by Bloom (1991) is used, for circumferential flaws. extending part way through the pipe wall, under combined tension and bending.

Both the fracture parameter $K_{r,a}$ and the plastic collapse parameter $L_{r,a}$ are functions of the crack depth and length at the time considered, as well as the applied tension and bending moment.

The following additional parameters are applied in the rupture analysis:

Ultimate tensile strength:
a normally distributed variable with mean value 584 MPa and coefficient of variation = 0.016.

Yield stress:
a normally distributed variable with mean value 493 MPa and coefficient of variation 0.014.

Material fracture toughness:
the Charpy impact energy C_v has a Weibull distribution with mean value 199 Nm and coefficient of variation 0.15. The fracture toughness in terms of stress intensity is given by

$$K_{mat} = \frac{51}{3}(C_v + 102) \quad \text{in N/mm}^{3/2}$$

Uncertainty in failure assessment curve:
found to be insignificant and discarded in analysis.

Plastic correction factor:
modelled according to PD 6493, (BSI, 1997), and found to be negligible.

Limit-State Formulation

The limit state function for failure mode (1), fatigue crack growth may simply be expressed by

$$g_1(t) = a_{cr} - a(t) \tag{12}$$

where t indicates elapsed time, a_{cr} is the critical crack depth, which is set equal to the tendon wall thickness, and $a(t)$ is the crack depth at that time. The accumulated probability of failure during T years is then

$$P[\text{fail while } t \le T] = P[G_1(T) < 0] \tag{13}$$

Naturally, the distributions of all the random variables have to be taken into account when computing this probability, although they are omitted for simplicity in this expression. Similarly, the marginal annual probability of failure in the year T, is given by

$$P[\text{fail while } T-1 < t \le T] = P[G_1(T) < 0] - P[G_1(T-1) < 0] \tag{14}$$

The limit state function for failure mode (2), rupture may be expressed by

$$g_2(t) = K_r(t) - K_{r,a}(t) \tag{15}$$

where $K_r(t)$ can be considered to be the "capacity" term, and is computed from equation (11) for the applied value of the plastic collapse parameter $L_r = L_{r,a}(t)$ and $K_{r,a}(t)$ is the applied stress intensity ratio, or "load" term. Visually, this corresponds to checking if the assessment point is above or below the failure assessment curve in Fig.4. This limit state function cannot be manipulated as freely as the previous one, because the loading now includes the stochastic load process itself, rather than the accumulated fatigue damage due to this process. The probability of failure can be formulated most accurately using vector out-crossing methods as described by Hagen and Sigurdsson (1994). However, these methods can be very computationally demanding. Alternatively, if we consider a short interval of time, we can approximately apply the crack size at the middle of that interval, together with the extreme value of the load process acting in the interval. This formulation is applied here, taking a year as a short time interval. Hence, the accumulated probability of failure during T years is given by

$$\begin{aligned} P[\text{fail while } t \le T] &= P[G_2(T) < 0 \cup G_2(T-1) < 0 \cup \ldots \cup G_2(1) < 0] \\ &= 1 - P[G_2(T) > 0 \cap G_2(T-1) > 0 \cap \ldots \cap G_2(1) > 0] \end{aligned} \tag{16}$$

where the time independent variables are common to all events, but the realisations of the annual extreme load are independent between events. Similarly, the marginal annual probability of failure in the year T, is given by

$$P[\text{fail while } T-1 < t \le T] = P[\text{fail while } t \le T] - P[\text{fail while } t \le T\text{-}1] \tag{17}$$

When evaluating these probabilities for large values of T, it is usually only necessary to consider the last few years, provided there is sufficient crack growth to significantly affect the annual probability of failure in consecutive years.

SELECTION OF ACCEPTANCE CRITERIA

Target reliabilities should, to the extent possible, be calibrated against well established cases that are known to have adequate safety. Existing codes for other types of offshore structures can be used to quantify a suitable target level for tendon inspection. In the NPD, *Act, regulations and provisions for the petroleum activities* (NPD 1996), the design factors are specified as follows for structural details with no access for inspection or repair:

Damage Consequence	No access or in the splash zone
Substantial consequence	10
No substantial consequence	3

(The regulations do not specify in detail which analysis methods should be associated with the application of these safety factors.)

The reliability levels at these time periods (one tenth, or one third of the design life) consequently correspond to the target reliability level for which a structural inspection is required according to the code. This approach will be used to determine the target levels in the current study.

A probabilistic SN-Fatigue model is used to determine the acceptable reliability level implicit in the NPD code. The F2 SN-curve for cathodic protected joints is applied (HSE 1995 & DNV 1984 CN 30.2). The results lead to the following recommended target annual failure probabilities

Damage consequence	Design factor	Target failure probability
Substantial consequence	10	$1.0 \cdot 10^{-5}$
No substantial consequence	3	$1.0 \cdot 10^{-3}$

The selected target reliability level is applied to a fracture mechanics analysis, and the question of transferability of probability levels may be raised. Without discussing this question in depth, we note that the fracture mechanics analysis applied here has not been calibrated against the S-N analysis. Experience indicates that such calibration eliminates a little conservatism (Lotsberg et al, 1999).

In order to recommend a target annual failure probability to be applied for Jolliet tendon an assessment of the consequence of a tendon failure is required. The first step in this assessment is to evaluate the effect of a missing tendon on the global platform response and the loads in the remaining tendons. In the context of evaluation with respect to criteria set by the NPD, this effect is sought under extreme environmental actions, corresponding to a 100-year return period. Only maximum tendon tension is considered here. A conservative estimate of the loads in the remaining tendons has been made with one tendon missing. The most heavily loaded tendon was still able to withstand the maximum loads, according to the DNV (1995) Classification Note on Buckling Strength Analysis. Hence, it follows that target annual failure probability of $1.0 \cdot 10^{-3}$ may be applied.

RESULTS

Two of the findings from the in-situ inspection have be selected to be considered in a probabilistic analysis. The selected findings are the largest of the surface flaws (both in length and depth), located at the inner surface, and the volumetric flaw indication. The volumetric flaw indication is conservatively modeled as a surface crack. The initial flaw sizes are set equal to the measured sizes. The considered cases:

Case	Surface of Origin	Flaw depth '*a*' (mm)	Flaw length '2*c*' (mm)	aspect ratio '*a/c*'
Fat-1	ID	4.78	17.8	0.54
Fat-2	VOL	1.21	127	0.02

First the fatigue limit state is considered. The pure fatigue failure event has been defined as a through thickness crack. The results from the probabilistic analysis are summarized in the following:

Service after 1. Insp. (yr)	Year	Case *Fat-1* Failure Probability		Case *Fat-2* Failure Probability	
		Acc.	Annual	Acc.	Annual
8	1999	$2.2\ 10^{-7}$		$3.7\ 10^{-4}$	
10	2001	$8.3\ 10^{-7}$	$3.8\ 10^{-7}$	$1.3\ 10^{-3}$	$4.7\ 10^{-4}$
12	2003	$2.3\ 10^{-6}$	$8.8\ 10^{-7}$	$2.3\ 10^{-3}$	$5.5\ 10^{-4}$
14	2005	$5.3\ 10^{-6}$	$1.7\ 10^{-6}$	$3.5\ 10^{-3}$	$6.2\ 10^{-4}$
16	2007	$1.1\ 10^{-5}$	$2.9\ 10^{-6}$	$4.9\ 10^{-3}$	$6.8\ 10^{-4}$
18	2009	$1.9\ 10^{-5}$	$4.6\ 10^{-6}$	$6.3\ 10^{-3}$	$7.3\ 10^{-4}$
20	2011	$3.1\ 10^{-5}$	$6.7\ 10^{-6}$	$7.8\ 10^{-3}$	$7.7\ 10^{-4}$

Based on the analysis results, the following observations can been made:

- The annual failure probability for case *Fat-1*, is very low; i.e. less than 10^{-5} in year 2012. The annual failure probability for case *Fat-2* is about two orders of magnitude higher than for case *Fat-1* (i.e. about 10^{-3}, and is relatively time independent).
- The case *Fat-2* is the most critical one. It should, however, be noted that this flaw indication has been characterised as a volumetric flaw, but in the analysis it has been conservatively assumed to be a surface breaking flaw.
- The uncertainty in the material parameter *C* is the main uncertainty source in case *Fat-1*, but for case *Fat-2* the uncertainty in the initial crack depth is the most important. The uncertainty in the initial crack size is due to the measurement uncertainty in the inspection tool. The effect of the sizing uncertainty has been studied. It was shown that by reducing the standard deviation in the sizing accuracy by 50%, the annual failure probability decreases by factor of 10 to 40. The applied value of 1.3 mm is considered as a conservative estimate, which might be reduced by more detailed study of the available documentation for the applied inspection tool.
- In the analysis so far, 30% increased normal stresses due to bending moment have been assumed. In order to study the effect of the bending moment, 15% and 45% increased normal stresses have also been studied. The effect of the normal stresses due to bending moment is higher for case *Fat-1* than for case *Fat-2*. By increasing the normal stresses due to bending moment by 15% the failure probability increases by one order of magnitude for case *Fat-1* and half an order of magnitude for case *Fat-2*.

So far, only pure fatigue growth has been considered, where failure is defined as the event that the crack depth exceeds the thickness. Now, the integrated event of fatigue crack grow and final fracture is considered. The annual probabilities of failure for the two cases are shown, as functions of time, in Fig. 5. In the figure, the probability of pure fatigue failure is also included for comparison purposes.
The most probable failure mode for case *Fat-1* is unstable fracture of a crack size close to the initial size. But for case *Fat-2*, the most probable failure mode is that the crack, almost grow through the thickness before rupture. The sensitivity analyses for the two cases have shown that the uncertainty in the annual extreme tension is the most important parameter for case *Fat-1*, but for the case *Fat-2* the uncertainty in the initial crack size and the fatigue crack growth are governing.
As can be seen the most critical one is case *Fat-2*; i.e. volumetric flaw indication, where the annual failure probability is relatively time invariant, about 10^{-3} in year 2010. The annual probability of rupture for case *Fat-1* is less than 10^{-5}.

CONCLUSIONS

A reliability analysis has been formulated for the tendons of the Jolliet TLP, to evaluate the probability of failure in any single welded joint between the pipe sections from which the tendons are constructed. Fatigue crack growth and final rupture have been combined. Input data from the original design, inspection reports, and in-service measurements have been applied. These data have been supplemented with conservative assumptions when detailed information has been lacking.

A target level of 10^{-3} has been selected for the annual probability of failure. This has been inferred from the NPD code, when considering details of offshore structures with no access for inspection, and when failure does not have substantial consequence. This category is selected because conventional analysis shows that the Jolliet platform can withstand the failure of one tendon.

The reliability analysis has been applied to the most unfavourable flaw indications found in the tendon joints, during the in-situ inspection of the tendons carried out from 1990 to 1991. One of these flaw indications is considerably more critical than the other cases. The annual probability of failure for this case is calculated to be about 4×10^{-4} in 1999, increasing relatively slowly to about 8×10^{-4} in 2010. This is less than the target level.

Hence, the analysis shows that further inspection of the tendon joint welds need not be carried out until after the year 2010. This corresponds to the end of the service life currently planned for the platform.

ACKNOWLEDGEMENT

This work has been carried at Det Norske Veritas, on behalf of Conoco Inc. The authors gratefully acknowledge the permission to publish this work. The material presented herein should not necessarily be taken to represent the views of either of these companies.

REFERENCES

API, (1987), "Recommended Practice for Planning, Designing, and Constructing Tension Leg Platforms," RP2T, 1st ed., Washington DC.

Combustion Engineering, Lumus Crest Inc., Earl and Wright, (1987), "Green Canyon Block 184 Field Development Project: Detailed Engineering, Global Analysis Report," March 1987.

Bloom, J.M., (1991), "Appendix J - The Deformation Plasticity Failure Assessment Diagram (DPFAD) Approach to Evaluation of Flaws in Ferritic Piping, Defect Assessment in Components - Fundamentals and Applications", ESIS/EGF9, Mechanical Eng. Publications, London 1991.

BSI (1997), PD 6493, "Guidance on methods for assessing the acceptability of flaws in fusion welded structures," draft, British Standards Institution.

DNV, (1984), "Fatigue Strength Analysis for Mobile Offshore Units," Classification Note no. 30.2, Det Norske Veritas, Høvik.

DNVS, (1993), "PROBAN Theory Manual," Det Norske Veritas SESAM AS, Høvik.

Hagen, Ø., Sigurdsson, G., (1994), "Fatigue and Final Fracture: Combined Failure Modes," 13th Offshore Mech. and Arctic Engng. Conf., Vol.2, pp.161-171, Houston.

Hein, W., Je., Wal,, C.J., Young, C.D., Parks, D.E., (1990), "Materials, Welding, and Fabrication for the Jolliet Projects," 22nd Offshore Tech Conf., paper no. OTC6361, Houston.

Hunter, A.F., Zimmer, R.A., Wang, W-J., Bozeman, J.D., Adams, C.J., Rager, B.L., (1990), "Designing the TLWP," 22nd Offshore Tech Conf., paper no. OTC6360, Houston.

HSE, (1995), "Guidance on design, construction and certification," Health and Safety Executive, London.

Koon, J.R., Langewis, C., (1990), "Jolliet: The Project," 22nd Offshore Tech Conf., paper no. OTC6359, Houston.

Lotsberg, I., Sigurdsson, G., Wold, P.T., (1999), "Probabilistic Inspection Planning of the Åsgard A FPSO Hull Structure with Respect to Fatigue," to be presented at 18th Offshore Mech. and Arctic Engng. Conf., St.John's, Newfoundland.

Lumus Crest / Earl and Wright, (1987a), "Conoco Green Canyon 184 TLWP, Tendon In-Place Dynamic Response."

Lumus Crest / Earl and Wright, (1987b), "Conoco Green Canyon Block 184 TLWP, Tendon Fatigue and Fracture Mechanics Analysis Report."

Mathisen,J. and Sigurdsson,G., (1996), "Fatigue and Final Fracture Reliability Analysis for TLP Tendons," Det Norske Veritas, report no. 96-3486, Høvik.

NORSOK, (1999), "N-004 Design of Steel Structures. Annex C. Fatigue Strength Analyses," Norwegian Technical Standardisation.

NPD, (1996), "Act, regulations and provisions for the petroleum activities," Norwegian Petroleum Directorate, Stavanger.

Raju I.S. and Newman J.C., (1981), "An empirical stress-intensity factor equation for surface crack," Engineering Fracture Mechanics, Vol 15, pp.185-192.

Raju I.S. and Newman J.C. (1986). "Stress-intensity factors for circumferential surface cracks in pipe and rods under bending and tension loads", Fracture Mechanics, Vol.17, AST, STP 905, pp. 709-805.

Shang-Xian, W., (1985), "Shape change of surface crack during fatigue growth," Engineering Fracture Mechanics, Vol. 22, pp.897-913.

Sigurdsson, G., Mathisen, J., (1998), "Pilot Study on the Tendon Joints of the Jolliet TLP," Det Norske Veritas, report no.98-0423, Høvik.

Sigurdsson G., Torhaug R., (1993), "Discussion of the Fatigue Crack Model used as Decision Basis for Probabilistic Inspection Planning," 1993 OMAE, Vol II, page 79-87.

Summary Report of Conoco Tendon Pipe; Grade X60TM 24" O.D. x 0.812" W.T, 6. Jan 1988, Sumitomo Metal Industries, Ltd, Kashima Steel Works.

Wybro, P.C., Bultema, S.C., Mueller, J.L., (1990), "Installation of the Jolliet Field TLWP," 22nd Offshore Tech Conf., paper no. OTC6362, Houston.

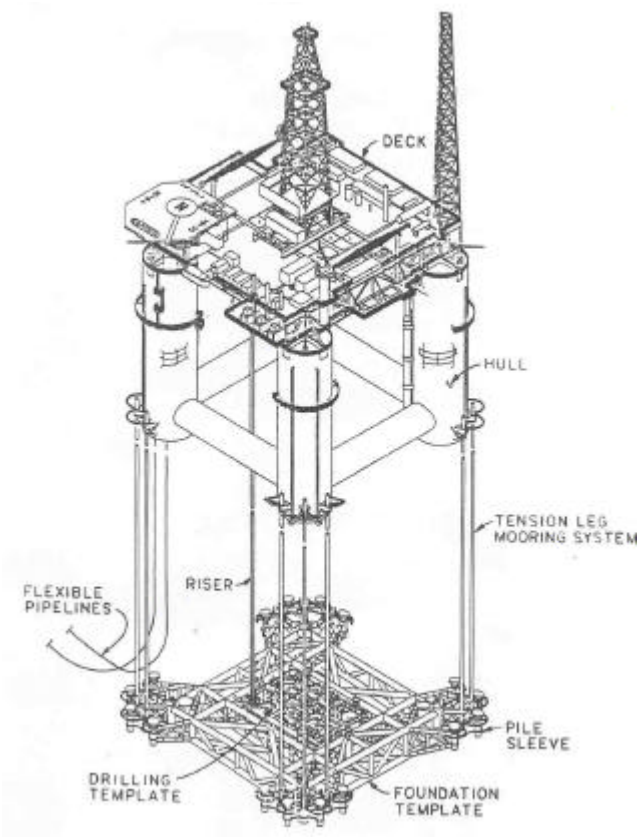

FIG. 1 THE TENSION LEG WELL PLATFORM, FROM HUNTER ET AL. (1990).

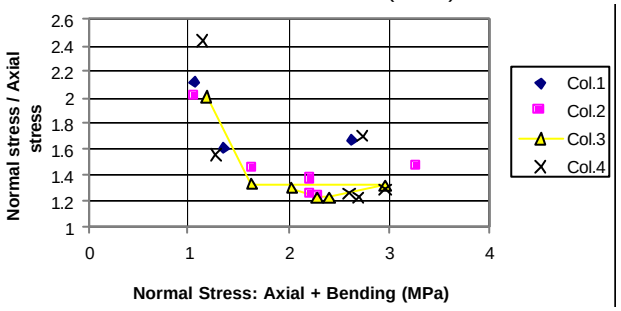

FIG.2 OSCILLATORY STRESS RATIO PLOTTED AGAINST NORMAL STRESS FROM SELECTED HOURS ON 25.08.92 AND 15.10.89 FOR ONE TENDON AT EACH COLUMN.

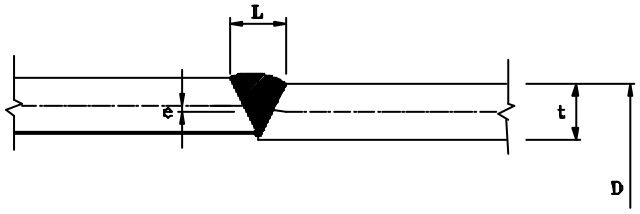

FIG.3 SECTION THROUGH WELD

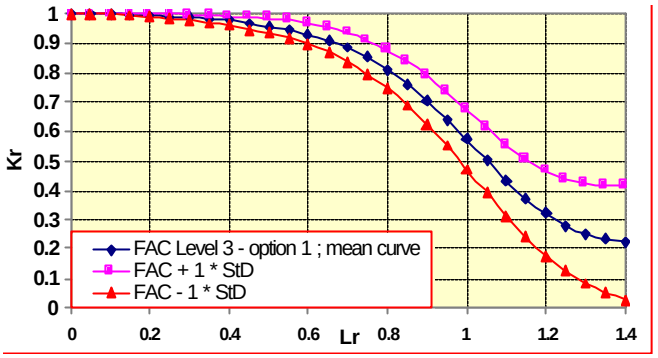

FIG. 4 THE EFFECT OF STOCHASTIC MODELLING OF THE FAILURE ASSESSMENT CURVE (FAC), MEAN CURVE ± 1 STD

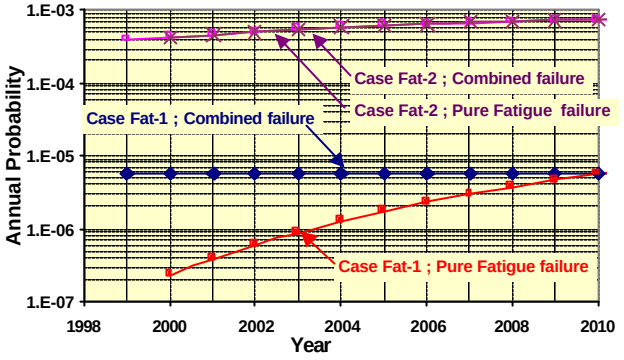

FIG. 5 ANNUAL FAILURE PROBABILITY FOR CASE FAT-1 AND FOR CASE FAT-2